HHS Public Access

Author manuscript

Cytoskeleton (Hoboken). Author manuscript; available in PMC 2020 June 10.

Published in final edited form as:

Cytoskeleton (Hoboken). 2018 December ; 75(12): 531–544. doi:10.1002/cm.21482.

Creation and testing of a new, local microtubule-disruption tool based on the microtubule-severing enzyme, katanin p60

Siddheshwari Advani[1], **Thomas J. Maresca**[1,2], **Jennifer L. Ross**[1,3]

[1]Molecular and Cellular Biology Graduate Program, University of Massachusetts Amherst

[2]Department of Biology, University of Massachusetts Amherst

[3]Department of Physics, University of Massachusetts Amherst

Abstract

Current methods to disrupt the microtubule cytoskeleton do not easily provide rapid, local control with standard cell manipulation reagents. Here, we develop a new microtubule-disruption tool based on katanin p60 severing activity and demonstrate proof-of-principle by targeting it to kinetochores in *Drosophila melanogaster* S2 cells. Specifically, we show that human katanin p60 can remove microtubule polymer mass in S2 cells and an increase in misaligned chromosomes when globally overexpressed. When targeted to the kinetochores via Mis12, we were able to recapitulate the misalignment only when using a phosphorylation-resistant mutant. Our results demonstrate that targeting an active version of katanin p60 to the kinetochore can reduce the fidelity of achieving full chromosome alignment in metaphase and could serve as a microtubule disruption tool for the future.

INTRODUCTION

Microtubules are comprised of alpha and beta tubulin heterodimers linked non-covalently into protofilaments that assemble into a hollow tube. Microtubule filaments form an essential network within cells, and the properties of the microtubule network can be modulated in response to external cues during various cellular processes, such as cell division, migration, and intracellular transport. In order for the cell to participate in these processes, they must control the nucleation, growth, and total polymer mass of microtubules in space and time. This is accomplished by modulating the inherent dynamics of the microtubules (dynamic instability) through microtubule associated proteins (MAPs) and enzymes.

Currently, methods to disrupt cellular microtubules at a particular location and time are limited and technically challenging. For instance, a number of spindle poisons act in distinct ways to alter the dynamic instability of the microtubule polymer and are frequently employed in anti-cancer therapies (extensively reviewed in [Jordan and Wilson, 2004]). These pharmacological agents either stabilize or inhibit all the microtubules in the cell. Taxol stabilizes the microtubule cytoskeleton against depolymerization [Arnal and Wade, 1995]. Vinblastine destabilizes the microtubule network by binding to tubulin dimers and inhibiting their incorporation into filaments [Gigant et al., 2005; Panda et al., 1996]. These pharmacological methods, while useful in grossly perturbing the microtubule cytoskeleton,

are limited in their ability to modify microtubules locally. Physical perturbations that are non-pharmacological include laser ablation. This method is technically challenging enough to be limited to a small group of expert laboratories. Further, laser ablation must be finely controlled and tuned so as to not damage other cellular structures and processes. Laser ablation is also limited to a small set of cell types.

The cell can locally control the microtubule network. Each distinct location of the cell, spatially separated by 10 to 1000 μm depending on cell type, can be mechanically and chemically distinct. The chemical and physical properties of the microtubule network in each location depends on cell type, stage in the cell cycle, or development. One particularly important role of microtubules occurs during mitosis. Even within this single process, microtubules display differential localizations, dynamics, and signaling. Astral microtubules help to keep the spindle localized within the cell volume [Kern 2016; Pease 2011; Giansanti 2001]. Kinetochore microtubules connect, localize, and apply forces to kinetochores to establish aligned chromosomes in metaphase [Waters 1996; Maiato 2004; Elting 2017]. And another set of microtubules that could either be a dense cloud of aligned, short filaments or overlapping interpolar filaments, fill in around the kinetochore microtubules (recently reviewed in [Orieola 2018]). The mitotic cell appears to control each of these microtubule networks locally, even then they are spatially overlapping. Such exquisite control highlights a need to be able to manipulate microtubules in a targeted manner, spatially and temporally.

Here, we used the microtubule-severing enzyme, katanin p60, as a local control knob on microtubule stability. Katanin p60 is a AAA+ ATPase from the meiotic clade of AAA enzymes [McNally and Vale, 1993; Frickey and Lupas, 2004]. When katanin p60 is incubated with Taxol-stabilized microtubules, internal breaks in the microtubule polymer, called severing events, were visualized [McNally and Vale, 1993; Diaz-Valencia et al., 2013; Bailey et al., 2015]. This process requires ATP to break the tubulin-tubulin bonds, and the tubulin released upon disassembly was demonstrated to be capable of re-polymerization via a microtubule pelleting assay [McNally and Vale, 1993].

Several previously demonstrated biochemical features of katanin p60 make it a strong candidate for use as a local microtubule-disruption tool. For instance, we have previously shown that the severing activity of katanin p60 is inhibited by high concentrations of free tubulin [Bailey et al., 2015]. Our result implies that a high concentration of katanin p60 is needed locally to elicit severing activity, and the subsequent release of large amounts of free tubulin dimers will turn off further severing activity. This provides an internal negative feedback loop to shut down severing after significant polymer loss. Such biochemical features need to be accounted for when using katanin p60 as a local microtubule-disruption agent. Specifically, high concentrations of katanin p60 will need to be localized to a specific region, but the disruption will be acute; not long term. The properties of katanin p60 make it a potentially useful microtubule-control tool.

Another layer of katanin p60 regulation is via post-translational modifications. A number of phosphorylation sites have been predicted for katanin p60 [Loughlin et al., 2011]. One of these phosphorylation sites was experimentally validated in a cross-species study by Loughlin et al [Loughlin et al., 2011]. They showed that Aurora B kinase-mediated

phosphorylation of Serine 131 on *Xenopus laevis* katanin p60 negatively regulates severing activity, thus acting as an additional means of control [Loughlin et al., 2011].

Our new microtubule-disruption tool uses the microtubule-destroying activity of katanin p60. The control occurs both chemically and spatially and can be visualized with fluorescent tags. Specifically, we have created a copper-sulfate inducible fusion construct with a fluorescent protein, TagRFP-T, for chemical induction and visualization. Further, we created and tested the activity of a chimeric construct to specifically localize katanin p60 to the kinetochore via fusion with Mis12 (Figure 1). Mis12 is a component of the Mis12 complex, that, together with the Ndc80 complex and KNL1 comprise the KMN network that mediates kinetochore interaction with spindle microtubules. In this techniques paper, we test the abilities of this novel microtubule-disruption scheme. We show that our new katanin-based tool can be successfully localized to the *Drosophila* kinetochore and remains active there.

REAGENTS AND INSTRUMENTS

All reagents and instruments can be found in the Supporting Information in Supplemental Table 1.

METHODS

CELL CULTURE

Drosophila S2 cells were grown at 24°C in Schneider's media (Life Technologies) containing 10% Heat-inactivated Fetal Bovine Serum (Life Technologies) and 0.5x antibiotic-antimycotic cocktail (Life Technologies).

PLASMIDS AND PROTEINS

Plasmids and constructs are shown in figure 1. Human katanin p60 was cloned from pMal-c2x MBP superfolder GFP human katanin [Bailey et al., 2015] into pMT-V5 His B TagRFP-T DmMis12 via Gibson cloning [Gibson et al., 2009] using the EcoRI site, generating pMT-V5 His B TagRFP-T DmMis12 HsKatanin p60 (TagRFP-T Mis12 katanin p60). The S131A mutation was made via site-directed mutagenesis using a modified version of the QuikChange XL protocol (TagRFP-T Mis12 katanin p60 S131A) [Qi and Scholthof, 2008]. The pMT-V5 His B TagRFP-T katanin p60 (soluble katanin p60 construct) was generated by deleting Mis12 from pMT-V5 His B TagRFP-T DmMis12 HsKatanin p60 using the Q5 Site-Directed Mutagenesis kit (NEB), and assembled with katanin p60 via Gibson assembly (TagRFP-T katanin p60). This construct was also mutated to have the S131A mutation as above (TagRFP-T katanin p60 S131A). Finally, we created a control construct without the TagRFP-T label or the Mis12 by assembling amplified HsKatanin p60 from pMT-V5 His B TagRFP-T katanin p60 wildtype vector with the pMT-V5 His B digested with KpnI and EcoRI via Gibson cloning (untagged katanin p60).

TRANSIENT TRANSFECTION OF *DROSOPHILA* S2 CELLS

Transient transfections of S2 cells were performed in a GFP-tubulin background using the Qiagen Transfection kit (Qiagen). GFP-tubulin S2 cells were plated at high density one hour

prior to transfection in a 35 mm tissue culture dish. Briefly, 1 μg of DNA was diluted with Buffer EC in a microfuge tube to obtain a final volume of 300 μl. This was mixed with 16 μl of Enhancer and incubated for 5 minutes. At the end of the incubation period, 60 μl of Effectene was added to the mixture and incubated for 10 minutes. One milliliter of complete S2 media was added to the tube, pipetted to mix, and added dropwise, replacing the existing S2 media in the dish. The dish was sealed with Parafilm and incubated at 24°C. The next day, 1 ml of complete media was added to the dish and sealed with Parafilm. On day 3, a small sample of cells were induced overnight with 500 μM $CuSO_4$. Cells were inspected for transfection efficiency and imaged on day 4.

GENERATION OF STABLE CELL LINES

Transiently transfected *Drosophila* S2 cells were treated with 25 μg/ml blasticidin and underwent 3–4 rounds of selection. Each round of selection was evaluated after induction. When no further increase in the ratio of expressing to non-expressing cells was seen, the cells were taken out of selection to make cryo-preserved stocks.

QUANTIFICATION OF MICROTUBULE POLYMER

Sample preparation and image acquisition: Cells were induced as described previously and plated at 50% confluency on ConA-coated, glass bottomed petri dishes (MatTek) for 20 min. Fresh pre-warmed media was added to the dish, and subsequently imaged on a spinning disk confocal microscope (Nikon Ti Eclipse) using a 100x oil immersion objective NA=1.49, at 2×2 binning and 0.2 μm Z-steps (ORCA Flash 4.0).

Live cells were visualized for GFP-tubulin using the 488 nm laser and TagRFP-T using the 561 nm laser. The exposures chosen for each of these wavelengths were 100 ms for the 488 nm laser, and 300 ms for the 561 nm laser, to minimize bleaching of the cells. The dish was imaged for a maximum of 1 hour. Chosen cells were well-separated from their neighbors, and a z-stack of images was taken to span the entire depth of the cell for both GFP and TagRFP-T channels (Supplemental Figure 1). The z-stack was used to create maximum projection images and reveal the location of the nucleus.

Fixed cells were visualized for GFP-tubulin and TagRFP-T by plating induced cells on ConA-coated coverslips. Cells were immunostained with anti-α tubulin antibody (DM1α, Millipore) followed by green secondary antibody to mouse (Alexa-488, 488 nm). TagRFP-T was imaged directly or stained with anti-TagRFP-T antibody followed by red secondary antibody to rabbit (Alexa-561, 561 nm). The exposures chosen for each of these wavelengths were 200 ms for the 488 nm laser, and 500 ms for the 561 nm laser. The coverslip was imaged within 1 week. Chosen cells were well-separated from their neighbors, and a z-stack of images was taken to span the entire depth of the cell for both GFP and TagRFP-T channels (Figure 2, supplemental figures 1, 2). Fixed cells displayed more background than live cells, and were only used to demonstrate (A) co-localization between TagRFP-T and katanin p60, or (B) identify cells that expressed katanin for the unlabeled katanin control (Supplemental Figure 2).

Image quantification: Files were imported into FIJI/ImageJ, and a maximum projection of the z-series was obtained for both channels (GFP-tubulin and TagRFP-T). To select only the microtubules in the field of view, the GFP channel was auto-thresholded and adjusted if needed to include the entire outline of the cell area. The Particle Analyzer command was run to add the thresholded areas to the region of interest (ROI) manager, generating outlines of the cells. Partial and conjoined cells were eliminated from the measurements. The ROI was used to measure the total area and total intensity of 16-bit, un-thresholded cells in the GFP and RFP channels.

To measure the intensity and area of microtubule polymer mass only, images of cells in the GFP channel were re-thresholded to only highlight microtubule polymer and exclude background tubulin intensity. This region was used to create an ROI. The Particle Analyzer command was run to add the thresholded areas to the ROI manager, generating outlines of the microtubule mass. The area and intensity of each ROI was measured on 16-bit, un-thresholded images to give the microtubule polymer area and intensity for the cell.

To measure the TagRFP-T signal in each cell, the TagRFP-T threshold was set to eliminate the background signal outside the cell and was found to be fairly constant across all images. The cell outline ROIs obtained from the GFP channel were transposed onto the TagRFP-T max projection to measure the TagRFP-T area and intensity. The thresholded image revealed the TagRFP area and intensity above background noise, and the un-thresholded image gave the TagRFP intensity and area of the entire cell.

The microtubule polymer intensity normalized to cell size was calculated as the ratio of the area occupied by thresholded GFP-microtubules to the total cell area. The same calculation was performed for TagRFP-T to determine the TagRFP-T intensity per cell area. To examine the microtubule polymer mass as a function of katanin p60 concentration, we plotted the microtubule polymer intensity (y-axis) as a function of the thresholded TagRFP-T intensity per cell area (x-axis). Three independent experiments were run to determine if there was a significant difference between the cells.

Statistical analysis: The normalized microtubule polymer mass and TagRFP-T signal were continuous variables between zero and one. Histograms of the data were not Gaussian distributions, so the student's t-test should not be used. We ran the Kolmogorov-Smirnov test to determine if the two distribution sets are statistically different. (http://www.physics.csbsju.edu/stats/KS-test.html). We determined the maximum difference between the cumulative distributions D, and compared this to the expected value of D at a given significance. If the distribution sets were found to have a D value smaller than the critical value of D at p=0.05, then the null hypothesis was accepted. If the two distribution sets had a D value larger than the critical value of D at p=0.05, we would reject the null hypothesis. Further, we used the Wilcoxon-Mann-Whitney test to evaluate the statistical significance of the data between expressing and non-expressing cells.

MISALIGNED CHROMOSOME ASSAY

Sample preparation and image acquisition: Stable or transiently transfected S2 cell lines were induced with 500 μM $CuSO_4$ overnight. Acid-washed coverslips were sterilized

and coated with ConA. The cells were plated onto ConA-coated coverslips placed in 35 mm dishes for 30 minutes at 50% confluency, treated with 20 μM MG132 in fresh S2 media for 1 hour, and subsequently processed for immunofluorescence.

Immunofluorescence: Coverslips were washed twice with BRB-80, fixed with 10% paraformaldehyde for 10 minutes, and permeabilized with PBS 1% Triton X-100 for 8 minutes. This method was used because it was the best at preserving the microtubule organization and the TagRFP-T signal. Coverslips were subsequently rinsed thrice with PBS 0.1% Triton X-100 and transferred onto a Parafilm sheet placed in a 150 mm dish. The coverslips were blocked with 5% Boiled Donkey Serum in PBS for 45 minutes. For most assays, we used primary antibodies to anti-α tubulin antibody (DM1α, Millipore) only. For examination of tubulin, katanin, and TagRFP-T localization, we used anti-GFP (Millipore), anti-TagRFP-T (Evrogen) and anti-human katanin p60 (Abveris). Primary antibodies were diluted in Boiled Donkey Serum at 1:1000 (DM1α or GFP), 1:5000 (anti-TagRFP-T), or 1:50 (anti-human katanin p60) and incubated with the coverslip for 1 hour at room temperature. The coverslips were washed thrice for five minutes each in PBS 0.1% Triton X-100, incubated with secondary antibodies diluted in Boiled Donkey Serum for 40 minutes to 1 hour, and washed again in the same manner with PBS 0.1% Triton X-100. The coverslips were stained with DAPI at a final concentration of 1 μg/ml in 5% Boiled Donkey Serum and washed thrice for 5 minutes each with PBS 0.1% Triton X-100. The coverslips were mounted in a glycerol-based Mounting Media and sealed with nail polish. The slides were stored at 4°C. TagRFP-T fluorescence was preserved in this manner for up to three weeks.

Scoring: A Nikon Ti Eclipse widefield microscope was used to visualize DNA using DAPI (405 nm), GFP-tubulin or secondary antibody on immunostained tubulin (488 nm), and TagRFP-T (561 nm). Cells were scored as misaligned if their chromosomes were more than 50% of the distance between the spindle pole and the metaphase plate. As is common with S2 cell cultures, ~50% of the cells do not express the protein of interest, and provide an internal control for our experiments.

Statistical analysis: The misaligned chromosome counts are discrete data with an integer number of misaligned chromosomes per cell. Histograms of the misaligned chromosome data for both katanin p60-expressing and non-expressing cells yield non-Gaussian distributions that cannot be evaluated using the student's t-test. Hence, we used the Chi square test to evaluate statistical significance. The degrees of freedom were calculated to be 1, and the Chi square value was evaluated and compared to the expected Chi-squared value at $p=0.05$, $p=0.01$, and $p=0.001$ significance levels. Chi-squared tests required that the number of cells in the control and experimental populations be equivalent. Often, the number of control cells was higher than those expressing. In order to compare the data, we rescaled the number of control cells both with and without misaligned chromosomes, so that the total number of control cells in the comparison population equaled the number of expressing cells measured (https://www.graphpad.com/quickcalcs/chisquared1.cfm).

RESULTS

We have created a microtubule-disruption tool using human katanin p60. Because high-level overexpression of katanin p60 leads to massive, global loss of microtubule polymer [Zhang et al., 2007], we needed to specifically localize the katanin p60 to a target region. Here, as a first test, we chose to localize the katanin p60 to the *Drosophila* kinetochore in S2 cells using Mis12 (Figure 1). This was a good and necessary first test for the following reasons. (1) *Drosophila* katanin p60 has been shown to localize to the spindle poles in S2 cells [Zhang et al., 2007]. Close inspection of the images from prior work showed that *Drosophila* katanin p60 was diffusely localized to the entire chromosome but was not specifically at the kinetochores [Zhang et al., 2007]. Thus, we reasoned that localizing katanin p60 to the kinetochores, where it could directly affect microtubule attachment to the chromosomes, could serve as a proof-of-concept. (2) Some types of katanin p60 have been shown to be regulated by kinase activity [Gomes et al., 2013; Quintin et al., 2003], specifically Aurora B kinase [Loughlin et al., 2011]. The kinetochore is a location with high levels of Aurora B kinase activity [Tanaka et al., 2002; Cheeseman et al., 2002]. Placing the katanin p60 tool within this region would allow us to test the control of microtubule-disruption via phosphorylation. (3) It has been previously shown that Mis12 could be modified with fusion proteins while still localizing and functioning at the kinetochore [Maldonado and Kapoor, 2011; Ballister et al., 2014; Ye et al., 2015]. Further, Mis12 localization to the kinetochores was microtubule-independent [Venkei et al., 2012; Kline et al., 2006]. Thus, if the katanin p60 locally destroyed the microtubules, we would expect that the Mis12 and katanin p60 would still reside at the kinetochore. Finally, Mis12 constitutively associated with centromeres throughout the cell cycle in *Drosophila* cells so Mis12-katanin p60 should localize to the nucleus during interphase [Venkei et al., 2012; Kline et al., 2006]

Here, we performed several tests of the abilities of human katanin p60 to serve as a microtubule-disruption tool in *Drosophila* S2 cells. We tested if human katanin p60 could act on *Drosophila* microtubules, if soluble katanin p60 had an effect on mitosis, and then compared these results to kinetochore-localized katanin p60.

Soluble Human Katanin p60 Reduces Microtubule Polymer in Interphase Drosophila Cells

We first needed to determine if human katanin p60 could act on *Drosophila* microtubules to disrupt the network. If functional, we expected that overexpression of the soluble human katanin p60 in S2 cells would lead to a decrease of *Drosophila* microtubule polymer mass. It was previously observed that over-expression of *Drosophila* katanin p60 was capable of removing the microtubule polymer mass in a dose-dependent manner [Zhang et al., 2007; Grode and Rogers, 2015]. We performed experiments with transient transfections of globally expressed TagRFP-T katanin p60 in S2 cells expressing GFP-α-tubulin (Figure 2). We imaged live cells in the GFP-microtubule polymer and TagRFP-T katanin p60 channels using a spinning disc confocal microscope. We subsequently quantified the levels of microtubule polymer mass and TagRFP-T expression, as described in the Methods.

Using maximum projection of z-stack images of live cells (Figure 2 A–C), we measured the area occupied by high-intensity GFP-microtubule polymer and the TagRFP-T signal, and normalized each to the total area of the cell. The microtubule polymer density (y-axis) was

plotted as a function of TagRFP-T expression (x-axis) on a scatter plot for all cells (Figure 2D). For non-expressing cells, the TagRFP-T signal consistently registered the same intensity as background levels, which is shown on the left side of the plot (Figure 2D, red boxes). Cells expressing TagRFP-T katanin p60 wildtype had a significantly higher katanin p60 concentration, and were consistently on the right side of the plot (Figure 2D, blue circles). We took the TagRFP-T data and plotted them using a box-whisker plot to demonstrate that there was significantly more katanin in the expressing cells (Figure 2E, $p < 0.0001$).

The distribution of the microtubule density fraction for non-expressing and expressing cells were plotted as box-whisker plots and shown to have significantly different distributions, with the mean and median significantly lower for the cells expressing TagRFP-T katanin p60 wildtype (Figure 2F). We used Kolmogorov-Smirnov (KS) and Wilcoxon-Mann-Whitney statistical tests and found that the polymer mass for expressing and non-expressing cells are distinct ($p < 0.0001$). These results are consistent with an interpretation that the TagRFP-T katanin p60 is able to actively reduce microtubule polymer, and is likely capable of severing and/or depolymerizing *Drosophila* microtubules in S2 cells.

We noted that some of the cells expressing high levels of TagRFP-T katanin p60 appeared to display aggregates of katanin. In all these cases, the background level of katanin was also relatively high, and the microtubule density was low. Such katanin aggregates were observed in a prior study that overexpressed *Drosophila* katanin in S2 cells [Zhang et al., 2007], and are likely a result of overexpression of a labeled katanin. In this prior study, cells displaying aggregates also showed reduced microtubule polymer mass (60% reduction) on average [Zhang et al., 2007]. Our experiments demonstrate a 94% reduction of the microtubule polymer mass, consistent with prior results. Although this prior study showed that cells with aggregates were able to reduce the microtubule polymer mass [Zhang et al., 2007], the intensity settings for the images published in the manuscript make it difficult to determine if there was a soluble pool of katanin in addition to aggregates.

Soluble Human Katanin p60 Leads to Misaligned Chromosomes in Mitosis

We next examined whether overexpressed soluble TagRFP-T human katanin p60 (Figure 1) altered mitosis in *Drosophila* S2 cells. If katanin p60 was widely affecting the process of mitosis, several phenotypes could be observed, including misaligned chromosomes, spindle length changes, large-scale spindle disorganization, or abnormal positioning of the spindle. There were no gross changes in mitotic spindle length or spindle morphology observed when wildtype (WT) human katanin p60 was overexpressed in S2 cells (Figure 3A–D). However, there was an increase in the percentage of metaphase-arrested S2 cells with ≥1 misaligned chromosomes upon global overexpression of WT human katanin p60. We found that 20 ± 3% of the overexpressing cells had misaligned chromosomes compared to 6 ± 1% in cells not expressing the construct in the same chamber (internal control) (Figure 3E). This 3.5 ± 0.9-fold change was significantly above 1-fold (Figure 3F), implying that overexpressed soluble WT human katanin p60 could alter mitotic microtubule dynamics in a manner that did not dramatically change spindle morphology, but did lead to a higher frequency of chromosome misalignment.

Soluble Non-phosphorylatable Katanin p60 Leads to Misaligned Chromosomes

The wildtype (WT) human katanin p60 tested above had a possible phosphorylation site at the same location in its sequence as *Xenopus laevis* katanin p60, serine 131 (predicted using GPS 3.0; www.gps.biocuckoo.org). A previous study on *Xenopus laevis* katanin p60 showed a serine site in the microtubule-binding domain (S131), when phosphorylated by Aurora B kinase, reduced the katanin p60 activity [Loughlin et al., 2011]. Phosphorylation of katanin p60 resulted in larger spindles in the frog oocyte and reduced severing *in vitro* [Loughlin et al., 2011; Whitehead et al., 2013]. First, we tested if a phosphomutant version of human katanin p60 made by replacing the serine at position 131 with an alanine (S131A, Figure 1) could reduce the microtubule polymer mass as well as soluble TagRFP-T katanin p60 WT. Using the same imaging and quantification of microtubule density and TagRFP-T signal, we found that cells expressing significantly distinct levels of TagRFP-T katanin p60 S131A were able to significantly reduce the microtubule polymer mass (Supplemental Figure 3, $p < 0.0001$).

Next, we tested the ability of the soluble TagRFP-T katanin p60 S131A to affect the mitotic spindle. We showed that global overexpression of WT human katanin p60 within mitotic cells caused misaligned chromosomes, but not other major morphological phenotypes. Because human katanin p60 could also be inhibited by phosphorylation in *Drosophila* S2 cells, we sought to determine if the minor phenotype was due to lower activity of WT katanin p60. We used transient overexpression of TagRFP-T katanin p60 S131A in S2 cells expressing GFP-tubulin and examined the changes in mitosis (Figure 4A–D). We did not observe gross morphological changes, spindle length changes, or major changes in spindle dynamics in these cells.

As with the wildtype (WT) katanin p60, there was an increase in misaligned chromosomes. We quantified the chromosomal misalignment for cells expressing soluble S131A katanin p60 mutant, relative to the internal control of non-expressing cells (Figure 4E). We found that the percentage of cells displaying misaligned chromosomes was 14 ± 2% for expressing cells compared to 5 ± 1% for non-expressing control cells in the same chamber (Figure 4E). The fold increase was 2.8 ± 0.7, which is significantly more than 1-fold, implying that this effect is truly caused by the katanin p60 expression (Figure 4F). The increase of chromosomal misalignment for katanin p60 S131A (2.8 ± 0.7) was within the uncertainty for the change for cells expressing katanin p60 WT (3.5 ± 0.9) (Figure 3F, 4F). Thus, soluble S131A katanin p60 led to the same level of misaligned chromosomes in mitosis as soluble WT katanin p60.

Kinetochore Localization of Mis12 Katanin p60

One issue with using a microtubule-severing enzyme as a microtubule-disruption agent is the global loss of polymer when it is ubiquitously overexpressed (Figure 2, Supplemental Fig 3). In our design scheme (Figure 1), the addition of the Mis12 fusion was meant to specifically localize the protein. Since Mis12 is constitutively localized to centromeres in flies [Venkei et al., 2012], overexpressed Mis12 katanin p60 should be localized to the nucleus during interphase. We needed to demonstrate that the overexpression of katanin p60 fused to Mis12 would not globally disrupt interphase microtubules. We used stable S2 cell lines that

expressed TagRFP-T Mis12 katanin p60 when induced by copper sulfate, as described in the Methods.

As with global expression of TagRFP-T katanin p60 WT, we imaged and quantified the GFP-microtubule polymer and TagRFP-T Mis12 katanin p60 signal (Figure 5A, B). The measured density of both the microtubule network and the TagRFP-T Mis12 katanin p60 were normalized by the size of the cell and plotted with TagRFP-T Mis12 katanin p60 signal on the x-axis and GFP-microtubule signal on the y-axis (Figure 5C). First, we noticed that the area density of TagRFP-T Mis12 katanin p60 was significantly reduced compared to the previously observed global expression of TagRFP-T katanin p60, with intensities about half that of the global expression (Figure 2D, 5C). Representing the TagRFP-T Mis12 katanin p60 density signal data as a box-whisker plot to show that there is still a significant increase in the TagRFP-T signal compared to non-expressing control cells in the same chamber (Figure 5D, $p < 0.0001$).

When comparing the TagRFP-T densities between global expression and Mis12 linkage, the Mis12 causes a significant loss of density ($p < 0.0001$ KS Test, Figure 2E compared to Figure 5D, blue bars). Close inspection shows that the TagRFP-T Mis12 katanin p60 was aggregated in cells in both the cell body and nucleus (Figure 5A, B). Unlike for TagRFP-T katanin p60, the addition of the Mis12 exacerbated aggregation such that there was barely detectable soluble pool of TagRFP-T Mis12 katanin p60. We suspect that katanin p60 in aggregates is not functional *in vivo*, and only the soluble pool is capable of destroying microtubule polymer in cells. This is based on our prior *in vitro* studies on katanin p60 activity, where highly concentrated preparations of katanin were observed to be inactive and had significant aggregation (unpublished data). We have since moved to a Maltose-Binding Protein affinity purification system that significantly reduces aggregation of purified proteins and enhances the activity of the purified katanin [Loughlin et al., 2011]. Our results suggest that katanin aggregates observed in cells occur as a consequence of high concentration of katanin and is increased due to the tethering to Mis12. In cells that only have aggregates, the microtubules remain without observable loss of polymer. In cells with a significant soluble pool of TagRFP-T katanin p60 in addition to aggregates, the microtubule polymer mass is significantly reduced (comparing Figure 5A,B to Figure 2B,C).

We quantified the microtubule network signal data and represented it as a box-whisker plot to highlight that we observed no significant difference in the microtubule polymer between TagRFP-T Mis12 katanin p60 WT expressing and non-expressing cells (Figure 5E, $p = 0.48$ using the Wilcoxon-Mann-Whitney test). We also used the KS Test and found the relative area fraction for expressing cells (median = 0.88, standard deviation = 0.14, N=143) and non-expressing cells (0.90, standard deviation = 0.11, N=185), were statistically indistinguishable ($p = 0.096$). This is not surprising given that the TagRFP-T Mis12 katanin p60 WT was all aggregated in these cells with no soluble katanin pool. We had hoped that the Mis12 would localize the TagRFP-T Mis12 katanin p60 WT to the nucleus to inactivate it during interphase. Instead, the Mis12 helped to aggregate the katanin p60, which may have sequestered and inactivated its microtubule destruction abilities. Despite not working as we expected, the result is as desired for a targeted microtubule-disruption tool.

We have demonstrated above, that our microtubule-disruption tool, when localized to the Mis12 complex, does not globally disrupt the microtubule network in interphase. We next wanted to test if the TagRFP-T Mis12 katanin p60 WT construct is localized to the kinetochore in mitosis. We expected that fusing katanin p60 to Mis12 would localize to the kinetochore during mitosis. Using immunofluorescence staining with antibodies against TagRFP-T, GFP-tubulin, and human katanin p60, we observed both the N-terminal TagRFP-T and the C-terminal katanin p60 signals overlap at the kinetochore (Figure 5F). This indicated that a full-length fusion protein was expressed and localized to the *Drosophila* kinetochore.

Overall, these results inform us that our TagRFP-T Mis12 katanin p60 microtubule disruption tool does the following. First, the human katanin p60 construct was active in S2 cells and could remove fly microtubules (Figure 2, 3). Second, the Mis12 fusion could inactivate katanin p60 in interphase to keep the tool sequestered and away from interphase microtubules (Figure 5). In mitosis, the Mis12 fusion localized human katanin p60 to kinetochores (Figure 5F).

Mis12 Katanin p60 Activity at Kinetochores During Mitosis

We have demonstrated that Mis12 can drive localization of human katanin p60 to the *Drosophila* kinetochores (Figure 5F). Next, we tested if human katanin p60 was active at the kinetochores. Active human katanin p60 at this position could have a variety of effects. We directly imaged stable S2 cells expressing inducible WT human katanin p60 fused to Mis12 during mitosis (Figure 6A–D). We did not find any large changes to spindle architecture upon inspection.

Above, we found that soluble katanin p60 was able to induce a chromosomal misalignment phenotype. Since there were no gross morphological changes, it is possible that TagRFP-T Mis12 katanin p60 WT protein localized to the kinetochores could also cause a chromosomal misalignment. When we quantified the misalignment of chromosomes for cells expressing TagRFP-T Mis12 katanin p60 WT protein, we found no significant change in misaligned chromosomes, 7 ± 2%, compared to the non-expressing cells, 5 ± 1% (Figure 6E). This change was a minor 1.4 ± 0.4-fold increase, indistinguishable from a 1-fold change (Figure 6F). We performed Chi-squared statistical analysis ($\chi^2 = 0.557$, degrees of freedom = 1) and found no difference between these results, as expected, given the uncertainty values we measured. We concluded that the WT katanin p60 placed at the kinetochore via Mis12 does not cause a chromosome misalignment phenotype.

The lack of an effect on chromosome alignment or spindle morphology with the TagRFP-T Mis12 katanin p60 WT construct was most likely due to local inhibition of human katanin p60 by Aurora B kinase emanating from centromeres. As described above, the S131 site is a target for Aurora B kinase in *Xenopus* p60. In order to determine if our katanin p60 tool was affected by Aurora B kinase, we created a point mutation where serine at amino acid 131 was mutated to alanine (S131A) (Figure 1). Since this construct could not be phosphorylated at that amino acid residue, the TagRFP-T Mis12 katanin p60 S131A should retain activity at kinetochores.

To test if human katanin p60 localized to the kinetochores is being turned off by Aurora B kinase, we produced a stable cell line expressing an inducible TagRFP-T Mis12 katanin p60 S131A. We first quantified the microtubule density as a function of TagRFP-T density in cells during interphase (Supplemental Figure 4). We found that the expression levels, aggregation, and inability to destroy microtubules globally during interphase was identical for the S131A version as it was for the wild type version of TagRFP-T Mis12 katanin p60 (Supplemental Figure 4).

Next, we tested the ability of TagRFP-T Mis12 katanin p60 S131A to alter chromosome alignment using widefield microscopy (Figure 7A–D). We observed a significant increase in cells with misaligned chromosomes for the Mis12 katanin p60 S131A-expressing cells, 22 ± 4%, relative to the internal control of non-expressing cells in the same chamber, 10 ± 3% (Figure 7E). The katanin p60 S131A localized to the kinetochores caused a 2.3 ± 0.7-fold increase in chromosomal misalignment, which is significantly different from a 1-fold change (Figure 7F). These results imply that the human katanin p60 can be inhibited by Aurora B kinase-mediated phosphorylation at S131, and that phosphorylation significantly reduces the activity of the kinetochore-targeted human katanin p60 in S2 cells. Further, the fact that TagRFP-T Mis12 katanin p60 WT did not result in an increase in chromosome misalignment means that the katanin p60 is effectively targeted to the kinetochore and turned off, since global expression of the WT katanin p60 resulted in chromosome misalignment. Our results imply that we have successfully created and targeted a microtubule-disrupting tool to the kinetochore.

DISCUSSION

Cells display a diversity of microtubule networks, even within the same cell or cellular apparatus. The filaments within these networks can have different lengths, stabilities, and crosslinkers. The organization of the filaments within the networks of a single cell can be parallel bundled, antiparallel bundled, astral, and disorganized. Each of these network organizations can perform a different function locally, and the disruption of an individual microtubule network, while leaving the rest intact, is a desirable experimental tool.

A recent study from the Wittman lab also sought to create a microtubule dynamics tool using light-activated EB proteins [van Haren et al., 2018]. Such modern local manipulation techniques are desirable compared to current microtubule manipulations that rely on global microtubule disruption via either cold temperature or pharmacological treatments. One feature of the EB technique is the use of light activation to specifically dial in the local cellular region for microtubule manipulation. Indeed, we foresee that the katanin p60 targeting system could also take advantage of such a light-activated localization scheme. For such a tool to work, the global level of katanin p60 would need to be low, so as not to destroy the entire microtubule cytoskeleton. The light activation scheme could localize exogenous katanin p60 to a specific region to cause local microtubule disruption. This could be done through either protein-based light-activation schemes (i.e. LOV proteins) or small molecule binding activities [Ballister et al., 2015; Zhang et al., 2017], using modern genetic manipulations (CRISPR-Cas) to obtain these cell lines. Importantly, our work here demonstrated that katanin p60, linked to other localization proteins, is still active. We could

easily attach the katanin p60 to Halo, LOV, or other proteins domains required for light-induced localization. Future manipulations of our initial katanin p60 tool could begin to address important questions of microtubule regulation in live cells.

Here, we have created and quantitatively characterized a new microtubule-disruption tool based on katanin p60 specifically localizing to a region of the cell. We have localized human katanin p60 to the kinetochore of *Drosophila* S2 cells as a first test. We showed that soluble human katanin p60 can significantly reduce the polymer density of fly microtubules, possibly by a combination of severing and depolymerization. This data is consistent with a microtubule-removing tool that is usable in a cross-species environment. We demonstrated that Mis12, a kinetochore complex protein, can localize katanin p60 to the kinetochores in mitosis and sequester katanin p60 to the nucleus during interphase. When placed at the kinetochore, human katanin p60 can be turned off by the Aurora B kinase phosphorylation site at S131. The inhibition can be overridden using the non-phosphorylatable mutant S131A, and katanin p60 is shown to be active at the kinetochore by causing a significant increase in chromosome misalignment.

Although we have only characterized our tool in this initial study at the kinetochore, there are a variety of other locations and binding partners that could be interesting to locally destroy microtubules. For instance, a tau-katanin p60 fusion could specifically target and enhance severing of axonal microtubules. A fusion with an Endoplasmic Reticulum (ER) surface protein could address the importance of the release of non-centrosomal microtubules that are nucleated at the ER. An added benefit of our copper-sulfate inducible expression is that protein expression levels can be titrated by controlling the amount of copper sulfate added. For experiments to examine processes during interphase, the levels of total katanin p60 could stay low, while the targeted katanin p60 could still have a locally high concentration that is required for its microtubule-disrupting function.

Further, our katanin p60 localization tool could also illuminate the physiological function of katanin p60. In our study, for instance, we have found new scientific knowledge about human katanin p60 and its effects in mitosis in S2 cells. Specifically, we found that human katanin p60 was inhibited when near the chromosomes. The most likely mechanism is for it to be inhibited by the Aurora B kinase, similar to the *Xenopus* katanin p60 [Loughlin et al., 2011]. Further the presence of additional, active katanin p60 does not affect spindle length in S2 cells. This is distinct from previous work that reported katanin p60 was important for meiotic spindle scaling in *Xenopus* egg extracts [Loughlin et al., 2011]. Our results support prior findings that Aurora B kinase activity inhibits katanin p60 [Loughlin et al., 2011]; our new findings suggest that spindle length is predominantly regulated by other mechanisms in S2 cells since soluble katanin p60 over-expression (either WT or S131A) did not change spindle length (Figure 3–4).

Another interesting finding is that, when katanin is placed at the kinetochores by Mis12, there is not a significant qualitative effect on either kinetochore fibers or gross morphological or dynamical changes to the spindle. This result is similar to a prior study on a different, highly potent microtubule destabilizer, Kif2C, a kinesin-family microtubule depolymerizing enzyme. This prior work showed that ectopic localization of Kif2C to the

centrosome was able to alter the dynamics of kinetochore microtubules; specifically, flux was depressed, and kinetochore fiber turn-over was enhanced [Manning et al., 2007]. Sister chromatid spacing and coordination was also adversely affected by excess depolymerizing kinesin at the centrosome [Manning et al., 2007]. This paper showed that the localization of a potent microtubule destabilizer near the microtubule-chromosome connection point can have subtle effects.

Many studies of katanin p60 severing activity and regulation have been performed *in vitro* by our group and others [Vale, 1991; McNally and Vale, 1993; Zhang et al., 2011; Bailey et al., 2015; Díaz-Valencia et al., 2011]. Whereas previous *in vivo* studies on katanin p60 have been largely limited to whole cell knockdowns [Zhang et al., 2007, 2011; Grode and Rogers, 2015; Jiang et al., 2017], a targeting tool for katanin p60 could enable quantitative biochemical and biophysical measurements in live cells with control over local concentration of katanin p60, *in situ*. Future experiments will permit a high degree of spatial and temporal control of katanin inside living cells.

Supplementary Material

Refer to Web version on PubMed Central for supplementary material.

ACKNOWLEDGEMENTS

This work was funded by the NIH R01 GM109909 grant to Jennifer L. Ross, the NIH R01 GM107026 grant to Thomas J. Maresca, and a Dissertation Research Grant from UMass Amherst to Siddheshwari Advani. The authors would like to thank Abveris for the anti-human katanin p60 antibody.

REFERENCES

Ahmad FJ, Yu W, McNally FJ, Baas PW. 1999 An essential role for katanin in severing microtubules in the neuron. J Cell Biol 145: 305–15. [PubMed: 10209026]

Arnal I, Wade RH. 1995 How does taxol stabilize microtubules? Curr Biol 5: 900–908. [PubMed: 7583148]

Bailey ME, Sackett DL, Ross JL. 2015 Katanin Severing and Binding Microtubules Are Inhibited by Tubulin Carboxy Tails. Biophys J 109: 2546–2561. [PubMed: 26682813]

Ballister ER, Ayloo S, Chenoweth DM, Lampson MA, Holzbaur ELFL. 2015 Optogenetic control of organelle transport using a photocaged chemical inducer of dimerization. Curr Biol 25: R407–R408. [PubMed: 25989077]

Ballister ER, Riegman M, Lampson MA. 2014 Recruitment of Mad1 to metaphase kinetochores is sufficient to reactivate the mitotic checkpoint. J Cell Biol. 204: 901–908. [PubMed: 24637323]

Cheeseman IM, Anderson S, Jwa M, Green EM, Kang J s, Yates JR, Chan CS, Drubin DG, Barnes G. 2002 Phospho-regulation of kinetochore-microtubule attachments by the Aurora kinase Ipl1p. Cell 111: 163–72. [PubMed: 12408861]

Díaz-Valencia JD, Bailey M, Ross JL. 2013 Purification and biophysical analysis of microtubule-severing enzymes in vitro. Purif. Biophys. Anal. Microtubule-Sev. Enzym. Vitro 115: 191–213.

Díaz-Valencia JD, Morelli MM, Bailey M, Zhang D, Sharp DJ, Ross JL. 2011 Drosophila katanin-60 depolymerizes and severs at microtubule defects. Biophys J 100: 2440–9. [PubMed: 21575578]

Frickey T, Lupas AN. 2004 Phylogenetic analysis of AAA proteins. J Struct Biol 146: 2–10. [PubMed: 15037233]

Gibson DG, Young L, Chuang R-Y, Venter CJ, Clyde AI, Smith HO. 2009 Enzymatic assembly of DNA molecules up to several hundred kilobases. Nat Methods 6: nmeth.1318.

Gigant B, Wang C, Ravelli RB, Roussi F, Steinmetz MO, Curmi PA, Sobel A, Knossow M. 2005 Structural basis for the regulation of tubulin by vinblastine. Nature 435: 519–22. [PubMed: 15917812]

Gomes J-E, Tavernier N, Richaudeau B, Formstecher E, Boulin T, Mains PE, Dumont J, Pintard L. 2013 Microtubule severing by the katanin complex is activated by PPFR-1–dependent MEI-1 dephosphorylation. J Cell Biol. 202: 431–439. [PubMed: 23918937]

Grode KD, Rogers SL. 2015 The Non-Catalytic Domains of Drosophila Katanin Regulate Its Abundance and Microtubule-Disassembly Activity. Plos One 10: e0123912. [PubMed: 25886649]

van Haren J, Charafeddine R, Ettinger A, cell … W-H. 2018 Local control of intracellular microtubule dynamics by EB1 photodissociation. Nat. Cell ….

Jiang K, Rezabkova L, Hua S, Liu Q, Capitani G, Altelaar AFMF, Heck AJRJ, Kammerer RA, Steinmetz MO, Akhmanova A. 2017 Microtubule minus-end regulation at spindle poles by an ASPM-katanin complex. Nat Cell Biol 19: 480–492. [PubMed: 28436967]

Jordan M, Wilson L. 2004 Microtubules as a target for anticancer drugs. 253–65.

Kline S, Cheeseman I, Hori T. 2006 The human Mis12 complex is required for kinetochore assembly and proper chromosome segregation.

Loughlin R, Wilbur JD, Francis JM, Nédélec FJ, Heald R. 2011 Katanin Contributes to Interspecies Spindle Length Scaling in Xenopus. Cell 147: 1397–1407. [PubMed: 22153081]

Maldonado M, Kapoor TM. 2011 Constitutive Mad1 targeting to kinetochores uncouples checkpoint signalling from chromosome biorientation. Nat Cell Biol 13: ncb2223.

Manning AL, Ganem NJ, Bakhoum SF, Wagenbach M, Wordeman L, Compton DA. 2007 The Kinesin-13 Proteins Kif2a, Kif2b, and Kif2c/MCAK Have Distinct Roles during Mitosis in Human Cells. Mol. Biol. Cell 18: 2970–2979. [PubMed: 17538014]

McNally FJ, Vale RD. 1993 Identification of katanin, an ATPase that severs and disassembles stable microtubules. Cell 75: 419–429. [PubMed: 8221885]

Panda D, Jordan M, Chu K, Wilson L. 1996 Differential effects of vinblastine on polymerization and dynamics at opposite microtubule ends. 271: 29807–12.

Qi D, Scholthof K-BG. 2008 A one-step PCR-based method for rapid and efficient site-directed fragment deletion, insertion, and substitution mutagenesis. J Virol Methods 149: 85–90. [PubMed: 18314204]

Quintin S, Mains P, Zinke A, reports H-A. 2003 The mbk-2 kinase is required for inactivation of MEI-1/katanin in the one-cell Caenorhabditis elegans embryo. EMBO Rep.

Sharp DJ, Ross JL. 2012 Microtubule-severing enzymes at the cutting edge. J Cell Sci 125: 2561–9. [PubMed: 22595526]

Tanaka T, Rachidi N, Janke C, Pereira G, Cell G-M. 2002 Evidence that the Ipl1-Sli15 (Aurora kinase-INCENP) complex promotes chromosome bi-orientation by altering kinetochore-spindle pole connections. Cell.

Vale RD. 1991 Severing of stable microtubules by a mitotically activated protein in xenopus egg extracts. 64: 827–839.

Venkei Z, Przewloka MR, Ladak Y, Albadri S, Sossick A, Juhasz G, Novák B, Glover DM. 2012 Spatiotemporal dynamics of Spc105 regulates the assembly of the Drosophila kinetochore. Open Biol 2: 110032. [PubMed: 22645658]

Whitehead E, Heald R, Wilbur JD. 2013 N-terminal phosphorylation of p60 katanin directly regulates microtubule severing. 425: 214–21.

Ye AA, Deretic J, Hoel CM, Hinman AW, Cimini D, Welburn JP, Maresca TJ. 2015 Aurora A Kinase Contributes to a Pole-Based Error Correction Pathway. Curr Biol 25: 1842–1851. [PubMed: 26166783]

Zhang D, Grode KD, Stewman SF, Juan DD-V, Liebling E, Rath U, Riera T, Currie JD, Buster DW, Asenjo AB, Sosa HJ, Ross JL, Ma A, Rogers SL, Sharp DJ. 2011 Drosophila katanin is a microtubule depolymerase that regulates cortical-microtubule plus-end interactions and cell migration. Nat Cell Biol 13: 361–70. [PubMed: 21378981]

Zhang D, Rogers GC, Buster DW, Sharp DJ. 2007 Three microtubule severing enzymes contribute to the “Pacman-flux” machinery that moves chromosomes. J Cell Biol. 177: 231–242. [PubMed: 17452528]

Zhang H, Aonbangkhen C, Tarasovetc EV, Ballister ER, Chenoweth DM, Lampson MA. 2017 Optogenetic control of kinetochore function. Nat Chem Biol 13: 1096–1101. [PubMed: 28805800]

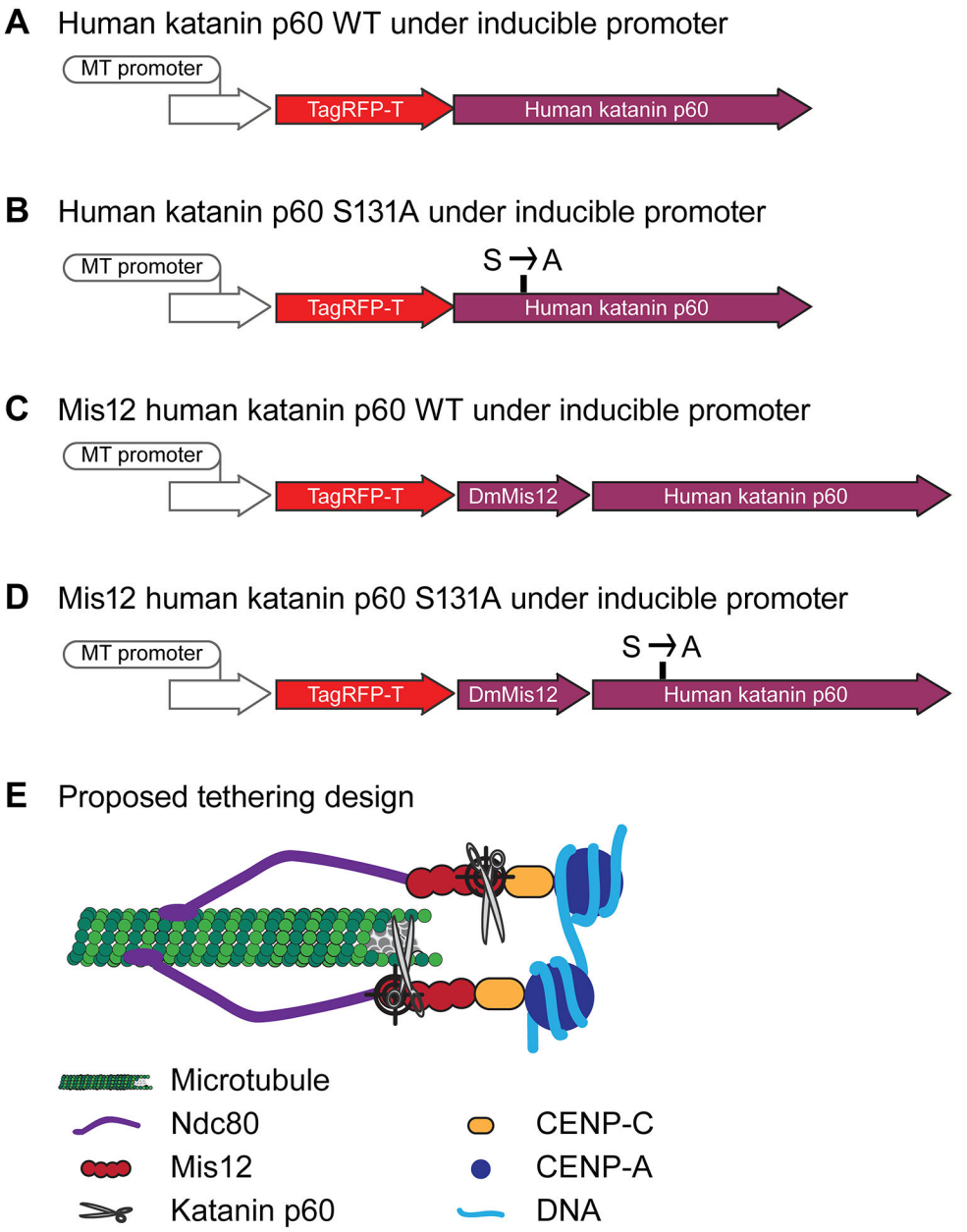

Figure 1: Constructs used in this study.

Constructs used in this study to create a microtubule disruption tool based on katanin p60. Each construct was made in pMT/V5-HisB plasmid with a Metallothionein (MT) promoter. (A) Human katanin p60 with TagRFP-T on the amino terminal end for global protein expression. (B) Human katanin p60 with serine to alanine mutation at amino acid 131 and TagRFP-T on the amino terminal end for global protein expression. (C) Chimera construct of drosophila Mis12, TagRFP-T, and human katanin p60 for localization at kinetochores. (D) Chimera construct of *Drosophila* Mis12, TagRFP-T, and human katanin p60 with serine to alanine mutation at amino acid 131 for localization at kinetochores. (E) Cartoon demonstrating the expected localization of chimeric constructs containing drosophila Mis12 and human katanin p60 at the kinetochore of S2 cells.

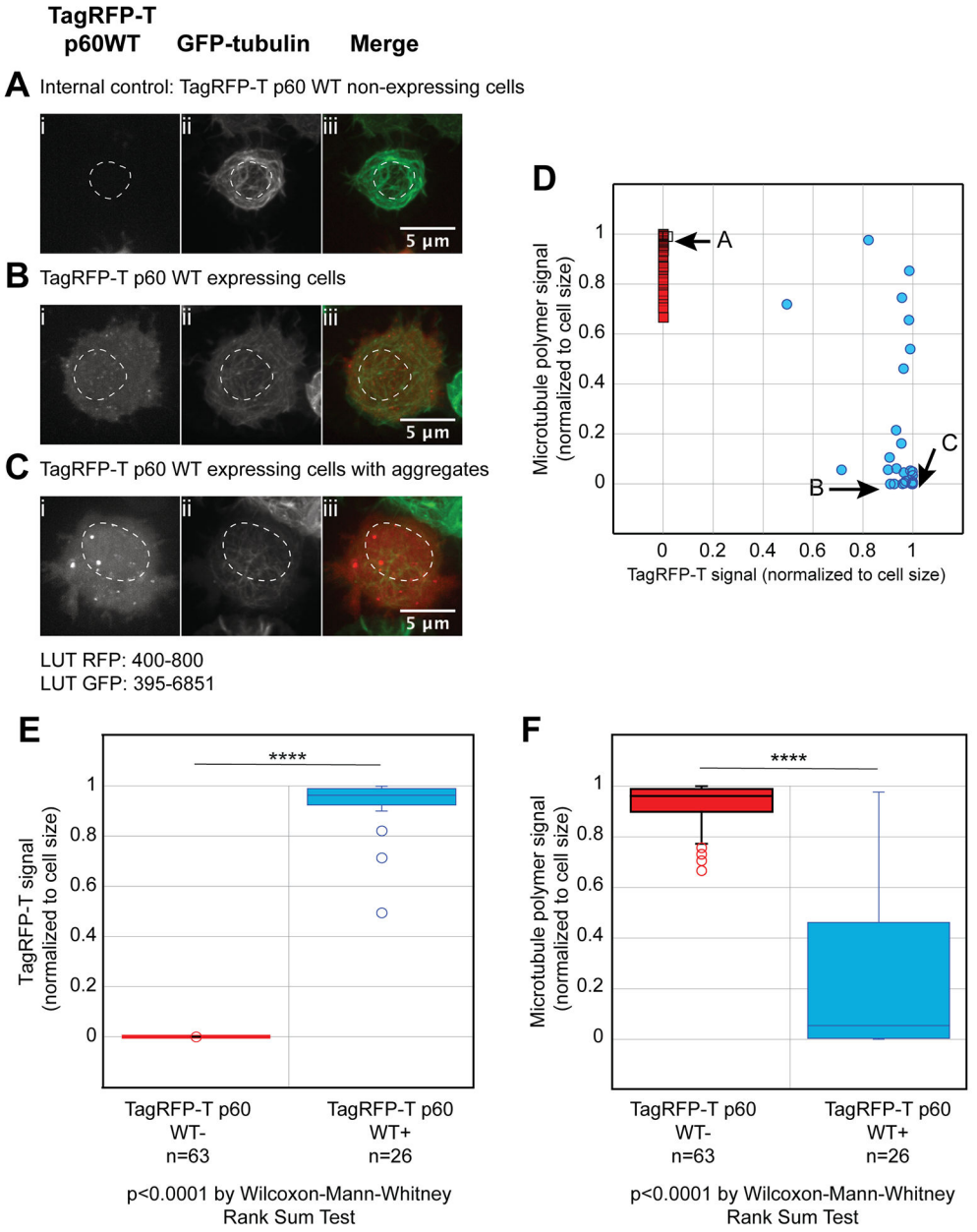

Figure 2: Quantification of TagRFP-T katanin p60 WT expression and microtubule polymer mass.

Live S2 cells transiently transfected with human katanin p60 WT were imaged to examine the GFP-microtubule polymer. **(A)** Example maximum projection of z-stack images with low expression of katanin showing **(i)** TagRFP-T katanin p60 WT signal with look up table (LUT) 400–800, **(ii)** GFP-tubulin signal with 395–6851 LUT settings. **(iii)** merged image of katanin (red) and microtubules (green). Position of the nucleus is shown using a dashed outline. **(B)** Example maximum projection of z-stack images with moderate expression of katanin showing **(i)** TagRFP-T katanin p60 WT signal with LUT 400–800, **(ii)** GFP-tubulin signal with 395–6851 LUT settings, **(iii)** merged image of katanin (red) and microtubules (green). Position of the nucleus is shown using a dashed outline. **(C)** Example maximum

projection of z-stack images with high expression of katanin showing **(i)** TagRFP-T katanin p60 WT signal with look up table (LUT) 400–800 and demonstrating the tendency for katanin to aggregate at high expression, **(ii)** GFP-tubulin signal with 395–6851 LUT settings, **(iii)** merged image of katanin (red) and microtubules (green). Position of the nucleus is shown using a dashed outline. **(D)** Scatter plot of normalized GFP-microtubule signal (y-axis) as a function of normalized TagRFP-T katanin p60 expression signal (x-axis). Cells in the chamber that were not expressing katanin (red squares) are on the left side (N = 63 cells in 1 experiments). Cells in the chamber that were expressing katanin (blue circles) are on the right side (N = 26 cells in 1 experiment). **(E)** Box-whisker plot of quantification of TagRFP-T katanin signal (x-axis values from part D) in the non-expressing cells (red box) and expressing cells (blue box). The difference between the expressing and non-expressing intensities are significant ($p < 0.0001$). **(F)** Box-whisker plot of quantification of GFP-microtubule signal (y-axis values from part D) in the non-expressing cells (red box) and expressing cells (blue box). The difference between the expressing and non-expressing intensities are significant ($p < 0.0001$).

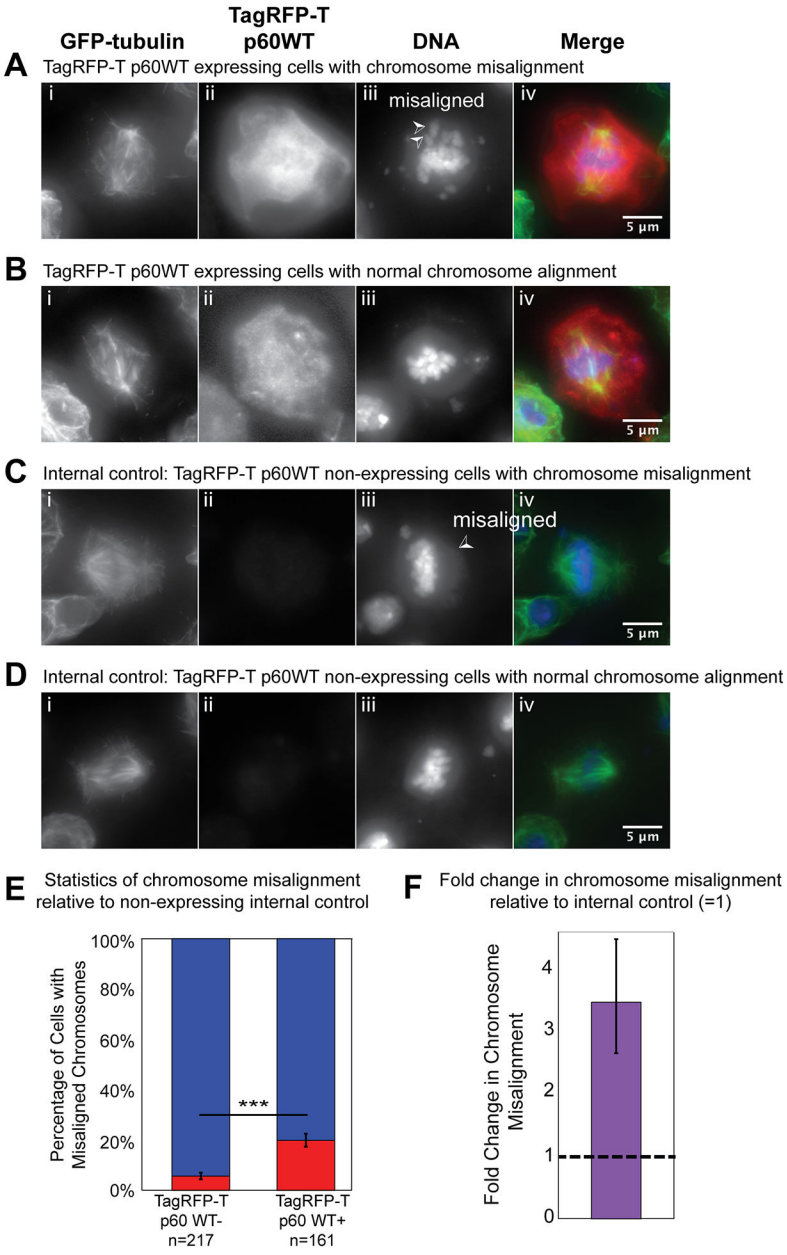

Figure 3: Quantification of misaligned chromosome frequency with soluble WT katanin p60.

S2 cells transiently transfected with katanin p60 WT were arrested in metaphase, processed for immunofluorescence, and scored. Maximum projections of z-stack images of cells expressing katanin p60 WT with a **(A)** misaligned chromosome and **(B)** normal alignment. Non-expressing (internal control) cells with **(C)** misaligned chromosome and **(D)** normal alignment. For each panel **(A-D)**, we display **(i)** GFP-tubulin channel, **(ii)** TagRFP-T katanin p60 WT channel, **(iii)** DNA stained with DAPI, and **(iv)** merge of GFP-tubulin, TagRFP-T katanin, and DNA. Scale bars are 5 μm for all frames. **(E)** Quantification of the incidence of misaligned chromosomes (red bars) compared to normal alignment (blue bars) in cells expressing soluble p60 WT (N = 161 cells, 3 chambers) was greater than that for non-expressing cells (N = 217 cells, 3 chambers). The difference is significant because the χ^2 =

55.1, with 1 degree of freedom (cut-off for significance at $p = 0.001$ was anything greater than 10.8). **(F)** Quantification of the fold change in misaligned chromosomes comparing expressing to non-expressing cells (purple bar). Error bars are accumulated measured uncertainty in the experiments. Dashed line indicates 1-fold change (no change).

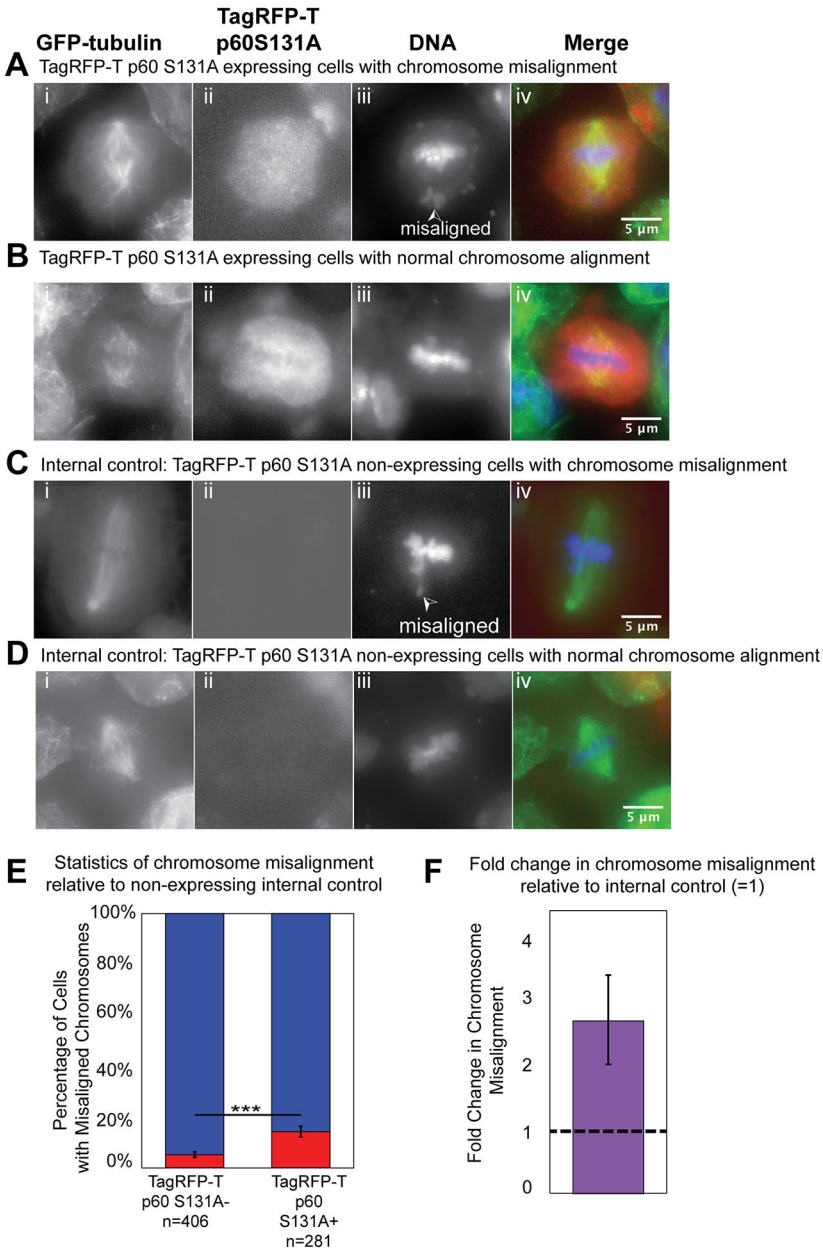

Figure 4: Quantification of misaligned chromosome frequency with soluble katanin p60 S131A.

S2 cells transiently transfected with katanin p60 with serine to alanine mutation at amino acid 131 (S131A) were arrested in metaphase, processed for immunofluorescence, and scored. Maximum projections of z-stack images of cells expressing katanin p60 S131A with a **(A)** misaligned chromosome and **(B)** normal alignment. Non-expressing (internal control) cells with **(C)** misaligned chromosome and **(D)** normal alignment. For each panel **(A-D)**, we display **(i)** GFP-tubulin channel, **(ii)** TagRFP-T katanin p60 S131A channel, **(iii)** DNA stained with DAPI, and **(iv)** merge of GFP-tubulin, TagRFP-T katanin, and DNA. Scale bars are 5 µm for all frames. **(E)** Quantification of the incidence of misaligned chromosomes (red bars) compared to normal alignment (blue bars) in cells expressing soluble p60 WT (N = 281 cells, 3 chambers) was greater than that for non-expressing cells (N = 406 cells, 3

chambers). The difference is significant because the $\chi^2 = 30.5$, with 1 degree of freedom (cut-off for significance at $p = 0.001$ was anything greater than 10.8). **(F)** Quantification of the fold change in misaligned chromosomes comparing expressing to non-expressing cells (purple bar). Error bars are accumulated measured uncertainty in the experiments. Dashed line indicates 1-fold change (no change).

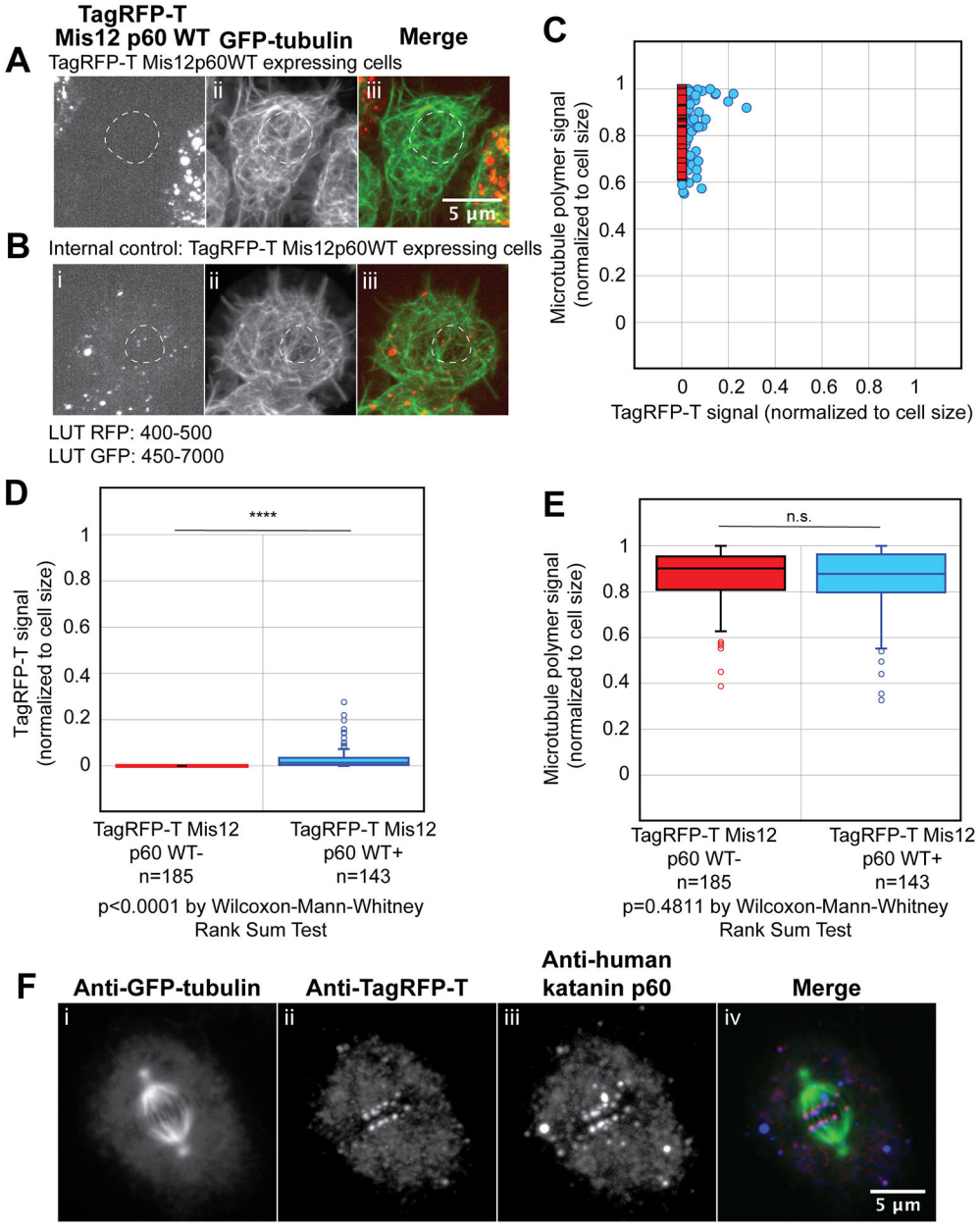

Figure 5: Quantification of TagRFP-T Mis12 katanin p60 WT and microtubule polymer mass in interphase and kinetochore localization in mitosis.

Live S2 cells stably expressing Mis12 TagRFP-T human katanin p60 WT were imaged to examine the GFP-microtubule polymer. **(A)** Example maximum projection of z-stack images with low expression of katanin showing **(i)** Mis12 TagRFP-T katanin p60 signal with 400–500 LUT, **(ii)** GFP-tubulin signal with 450–7000 LUT settings, **(iii)** merged image of katanin (red) and microtubules (green). Position of the nucleus is shown using a dashed outline. **(B)** Example maximum projection of z-stack images with moderate expression of katanin showing **(i)** Mis12 TagRFP-T katanin p60 WT signal with LUT 400–500, **(ii)** GFP-tubulin signal with 450–7000 LUT settings, **(iii)** merged image of katanin (red) and microtubules (green). Position of the nucleus is shown using a dashed outline. **(C)** Scatter plot of

normalized GFP-microtubule signal (y-axis) as a function of normalized Mis12 TagRFP-T katanin p60 expression signal (x-axis). Cells in the chamber that were not expressing katanin (red squares) are on the left side (N = 185 cells in 3 experiments) Cells in the chamber that were expressing katanin (blue circles) are on the right side (N = 143 cells in 3 experiment). **(D)** Box-whisker plot of quantification of TagRFP-T katanin signal (x-axis values from part C) in the non-expressing cells (red box) and expressing cells (blue box). The difference between the expressing and non-expressing intensities are significant ($p < 0.0001$). **(E)** Box-whisker plot of quantification of GFP-microtubule signal (y-axis values from part C) in the non-expressing cells (red box) and expressing cells (blue box). The difference between the expressing and non-expressing intensities is not significant ($p < 0.49$). **(F)** Immunofluorescence staining of fixed mitotic cell expressing TagRFP-T Mis12 katanin p60 shows localization of katanin to the kinetochores when stained for **(i)** GFP-tubulin, **(ii)** TagRFP-T, and **(iii)** human katanin p60. **(iv)** Merged images show overlap of the TagRFP and katanin signals with expected localization of kinetochore implying that the Mis12 is capable of localizing the katanin to the correct location during mitosis.

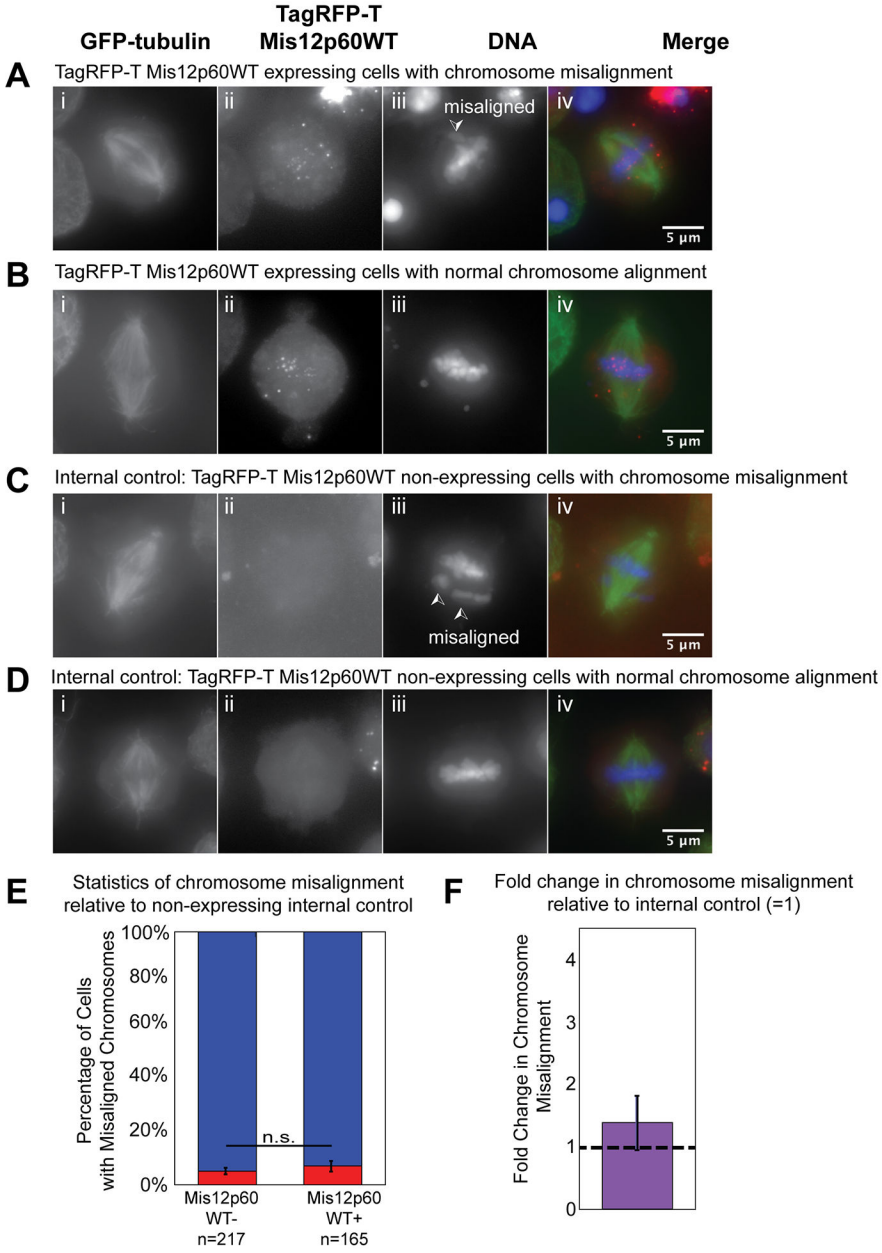

Figure 6: Quantification of misaligned chromosome frequency with Mis12-p60 WT.

S2 cells stably expressing TagRFP-T Mis12 WT katanin p60 were arrested in metaphase, processed for immunofluorescence, and scored. Maximum projections of z-stack images of cells expressing Mis12 katanin p60 with a **(A)** misaligned chromosome and **(B)** normal alignment. Non-expressing (internal control) cells with **(C)** misaligned chromosome and **(D)** normal alignment. For each panel **(A-D)**, we display **(i)** GFP-tubulin channel, **(ii)** Mis12 TagRFP-T katanin p60 channel, **(iii)** DNA stained with DAPI, and **(iv)** merge of GFP-tubulin, Mis12 TagRFP-T katanin, and DNA. Scale bars are 5 μm for all frames. **(E)** Quantification of the incidence of misaligned chromosomes (red bars) compared to normal alignment (blue bars) in cells expressing Mis12 TagRFP-T katanin p60 (N = 217 cells, 3 chambers) was the same as that for non-expressing cells (N = 165 cells, 3 chambers). The

difference is not significant because the $\chi^2 = 0.56$, with 1 degree of freedom (cut-off for significance at $p = 0.05$ was anything greater than 3.84). **(F)** Quantification of the fold change in misaligned chromosomes comparing expressing to non-expressing cells (purple bar). Error bars are accumulated measured uncertainty in the experiments. Dashed line indicates 1-fold change (no change).

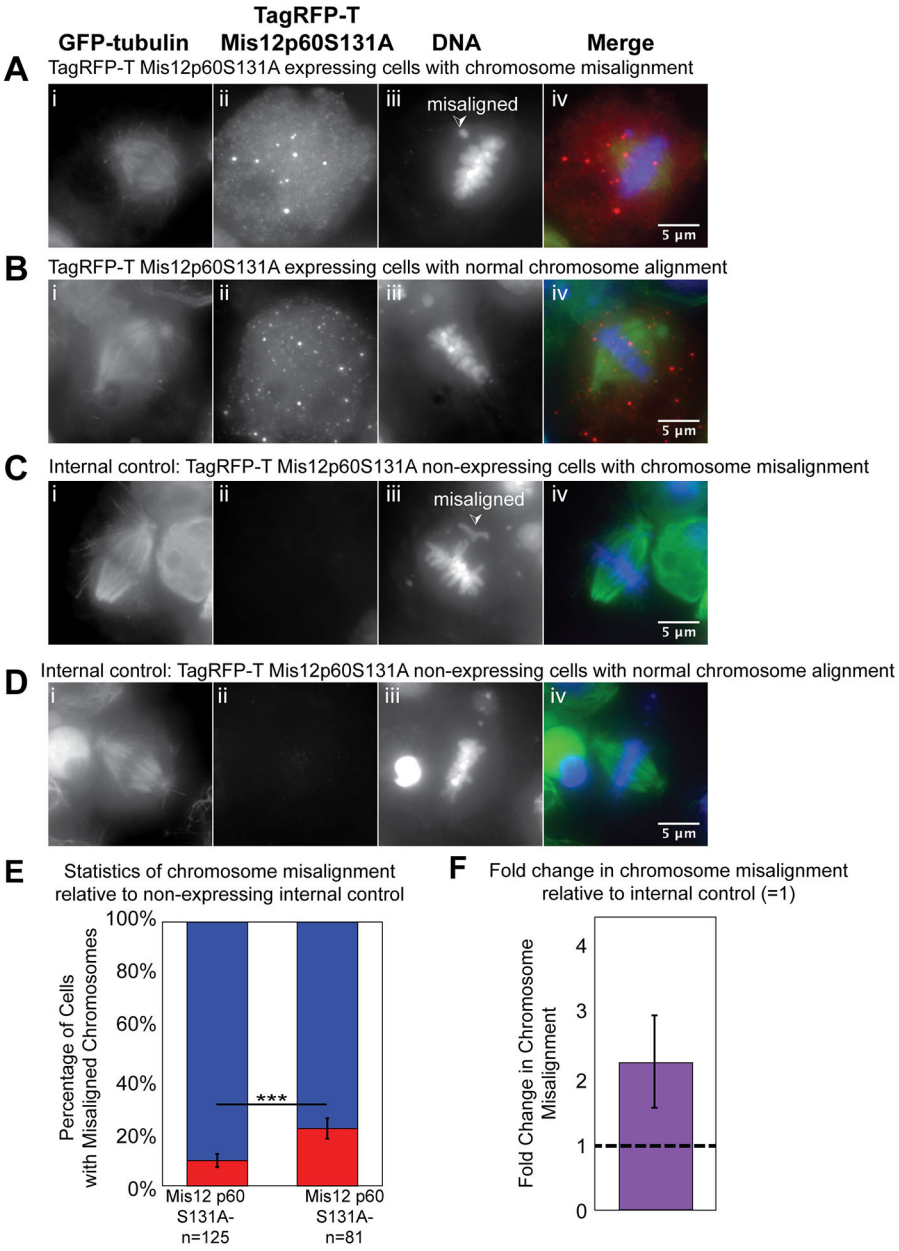

Figure 7: Quantification of misaligned chromosome frequency with Mis12-p60 S131A: A localized microtubule-disruption tool.

S2 cells stably expressing TagRFP-T Mis12 katanin p60 with an alanine to serine mutation at amino acid 131 (S131A) were arrested in metaphase, processed for immunofluorescence, and scored. Maximum projections of z-stack images of cells expressing Mis12 katanin p60 with a **(A)** misaligned chromosome and **(B)** normal alignment. Non-expressing (internal control) cells with **(C)** misaligned chromosome and **(D)** normal alignment. For each panel **(A-D)**, we display **(i)** GFP-tubulin channel, **(ii)** Mis12 TagRFP-T katanin p60 channel, **(iii)** DNA stained with DAPI, and **(iv)** merge of GFP-tubulin, Mis12 TagRFP-T katanin, and DNA. Scale bars are 5 µm for all frames. **(E)** Quantification of the incidence of misaligned chromosomes (red bars) compared to normal alignment (blue bars) in cells expressing

Mis12 TagRFP-T p60 S131A (N = 122 cells, 3 chambers) was greater than that for non-expressing cells (N = 115 cells, 3 chambers). The difference is significant because the χ^2 = 19.8, with 1 degree of freedom (cut-off for significance at p = 0.001 was anything greater than 10.8). **(F)** Quantification of the fold change in misaligned chromosomes comparing expressing to non-expressing cells (purple bar). Error bars are accumulated measured uncertainty in the experiments. Dashed line indicates 1-fold change (no change).